Available online at www.sciencedirect.com
SCIENCE DIRECT
Talanta 67 (2005) 908–917
Talanta
www.elsevier.com/locate/talanta

Single-crystal sapphire-fiber optic sensors based on surface plasmon resonance spectroscopy for in situ monitoring

Yoon-Chang Kim, Jean-Francois Masson, Karl S. Booksh *

Department of Chemistry and Biochemistry, Arizona State University, Tempe, AZ 85287-1604, USA

Received 22 February 2005; received in revised form 1 April 2005; accepted 4 April 2005
Available online 24 August 2005

Abstract

Single-crystal sapphire-fiber optic sensors based on surface plasmon resonance (SPR) for refractive index (RI) measurements of aqueous and hydrothermal water solutions are described. Accurate measurement of RIs is essential to efficient operation and control of broad range of engineering processes. Some of these processes are carried out with harsh environments, such as high-temperature, high pressure, and chemical corrosion. These extreme physical conditions are proving a limiting factor in application of the conventional silica-based optical sensors. Single-crystal sapphire is an ideal material for sensor applications, where reliable performance is required in the extreme environment conditions. With regard to the liquid species detection, most applications of SPR sensors are designed to function near the refractive index of water (1.3330 RI). The RI changes of aqueous solution can be easily monitored by silica-fiber (RI, 1.4601 at 550 nm) based SPR sensor. However, the sapphire waveguide has a prohibitively high RI (1.7708 at 546 nm) for unmodified monitoring of the RI changes of aqueous solutions. For that purpose, a practical SPR probe geometry has been applied to the ability to tune the SPR coupling wavelength/angle pair with sapphire-fiber based SPR probe.

Keywords: Fiber optic sensor; Surface plasmon resonance; Sapphire-fiber; Rapid thermal annealing

1. Introduction

The optical phenomenon of surface plasmon resonance (SPR) has many applications ranging from the analysis of biomaterials to environmental inspection. The technique of SPR is based on an electromagnetic phenomenon that is capable of monitoring refractive index (RI) [1,2] and thickness of the dielectric medium [3,4] that come into near contact with sensing surface. SPR sensing platforms are traditionally based on the Kretschmann configuration [5,6], consisting of a prism with thin layer of highly conductive metal (most often gold or silver) deposited onto one face to form the sensing surface. The reflection characteristics of a medium adjacent to the metal film are highly sensitive to RI variations in the sample medium.

Two main types of the SPR sensors have commonly been employed: constant-angle SPR (i.e., spectral SPR) and constant-wavelength SPR (i.e., angular SPR). In the prism-based SPR sensor, the surface plasmon wave (SPW) on the prism can be excited by light with a modulated angle of incidence. Otherwise, the reflected intensity can be measured by wavelength modulation while the incident angle is kept fixed and the wavelength of the incident light is changed. Therefore the prism-based SPR sensor system can be used either as a spectral or angular SPR sensor. The prism-based SPR sensors are not, however, optimal for in situ industrial or environmental process monitoring. The sensing region is by necessity more bulky that single fiber optics probe because of the rigid geometry of the sensor head. Thus, even the mini-Spreeta by Texas Instruments requires fluid handling systems to bring the sample to the sensor head instead of immersion of the sensor in the sample.

The use of optical fibers for the SPR sensing has recently attracted much attention [1,7–18] because the optical fiber

* Corresponding author. Tel.: +1 480 965 3058; fax: +1 480 965 2747.
E-mail address: booksh@asu.edu (K.S. Booksh).

0039-9140/$ – see front matter © 2005 Published by Elsevier B.V.
doi:10.1016/j.talanta.2005.04.022

sensors have several distinct advantages over the prism-based sensor. They are fundamentally simple in structure, less costly, require smaller sample volumes, and are amenable towards remote sensing applications. In the traditional fiber-based SPR sensor system, there is not a fixed incident angle but a range of angles that are allowed to propagate in the multimode fiber probe. The incident light consists of a wide range of wavelengths launched into the fiber in order to excite the SPW across a range of angles defined by the numerical aperature of the fiber optic waveguide. However, the SPR coupling wavelength can be tuned selectively by modifying the geometry of the probe tip [1,15–17]. The probe geometry allows the sensor to be easily placed into the sample of interest, and the orientation of the sensing region requires a minimal sample volume, making significant invasion of the sample unnecessary [17].

Development of fiber optic SPR sensors for RI monitoring applications where the RI of the media is far from the RI of the waveguide is not trivial. Most SPR sensors are designed with incident angles in the range of 70°–89° from normal to monitor samples within 0.1 refractive units of the waveguide. BK7, SF10, or silica substrates (RI ∼ 1.42) are employed for aqueous applications (RI ∼ 1.34). Straight sapphire rod (RI ∼ 1.77) has been employed for SPR sensors, but the application was the monitoring of epoxy curing processes (RI > 1.48) [18]. Such a range of applications translate well to fiber optic sensors, the angle of incidence is within the numerical aperature of the optical fiber and the distribution of angles propagated by the fiber do not result in an overly broad SPR spectral feature. However, to realize the sensitivity to refractive index changes greater than 0.1 refractive units less than the waveguide, the angle of incidence must approach 45°. Here two problems mutually compound to prohibit direct use of optical fibers. First, from the Fresnel equations, the angular sensitivity (change in SPR feature location with respect to change in angle) is greater the closer to normal the angle of incident becomes; thus to get a sharp spectral feature, strict control of incident light collimation must be realized. Second, to realize the acute angles of incidence in optical fibers, high numerical aperature fibers must be employed. However, the larger the numerical aperature results in a broader distribution of angle in the fibers. Even moderate numerical aperature fibers (0.22 or 0.39 NA) tapered, in the manner of Obando and Booksh [1], to present the appropriate angle of incidence yield SPR features so broad as to be useless when the RI of the media is far from the RI of the waveguide without redesign of the fiber optic SPR sensor platform.

Presented here are SPR monitoring applications where the RI of the media being monitored is significantly less than the RI of the waveguide. Single-crystal sapphire (RI ∼ 1.77) SPR probes are employed to monitor the density of aqueous solutions (RI ∼ 1.33). Here the ultimate application is the design of a fiber optic sensor to monitor fluid density in and around deep-sea hydrothermal vents. Seafloor hydrothermal vents, or "black smokers", have been discovered in many tectonically active areas of seafloor, at an average depth of ∼2100 m and in the both the Atlantic and Pacific oceans. In these regions, seawater seeps into cracks in the sea floor. This seawater is heated by the magma that lies beneath the earth's crust, and leaches minerals from the magmatic basalts. After a complex circulation, the hydrothermal fluids are emitted into the cold deep-sea water. These hydrothermal fluids are acidic, reduced and enriched with chemicals including heavy metals, methane and hydrogen sulphide. These near supercritical conditions of sulphide mineral-enriched water corrode most instrument platforms; sapphire, gold, diamond, and titanium are four of the few materials stable in these environments. To date, sensors for temperature, pH, H_2, and sulphide concentration have been the only successfully deployed instruments in hydrothermal vents [19–21]. The sapphire-fiber based SPR probe after the RTA treatment is highly desirable in a wide range of the engineering applications with harsh environments such as the natural seafloor hydrothermal vents, high-temperature combustion, and industrial processes monitoring of corrosive reagents. Additionally, the system could be applied to the development of advanced high-temperature materials.

2. Experimental

2.1. Probe designs

The fiber optic SPR system has been previously described [1]. The sensor system associated with the fiber optic SPR probe is shown in Fig. 1-1. A bifurcated 0.22 ± 0.02 numerical aperture optical fiber jumper was used to guide the light from the source, to the probe, and back to the detector. Polyimide clad fibers (Polymicro Technologies) having 200 ± 8, 220 ± 5 and 240 ± 5 μm core, cladding and buffer diameters, respectively, were employed to manufacture the jumper in house. A white light LED that can be operated over 100 h on a commercial 9 V household battery was employed for the source. Light from the LED was focused on the optical fiber with a SMA fiber optic coupling lens (Thor Labs). For the initial tests and the analyses with silica SPR probes, returned light from 502 to 950 nm was dispersed by a Kaiser Hollospec spectrograph (Kaiser Optical Systems Inc.) and collected on a Princeton Instruments CCD camera (Roper Scientific). For the analyses with sapphire SPR probes, a Jobin-SPEX 270 M spectrometer with 1800 gr/mm grating was used to narrow the spectral range to 42.8 nm. The spectra were collected with 1024×256 pixels Andor CCD camera.

Three different types of optical fibers for SPR probes were employed in these experiments. All three optical fibers were selected to be approximately 400 μm in core diameter to maximize the coupling between the probe tip and the bifurcated fiber jumper. Single-crystal sapphire optical fibers (Photran, LLC) were 425 μm in diameter and did not have a cladding or buffer. Silica core optical fibers with 0.39 NA were employed. The 0.39 NA multimode fibers (Thor labs)

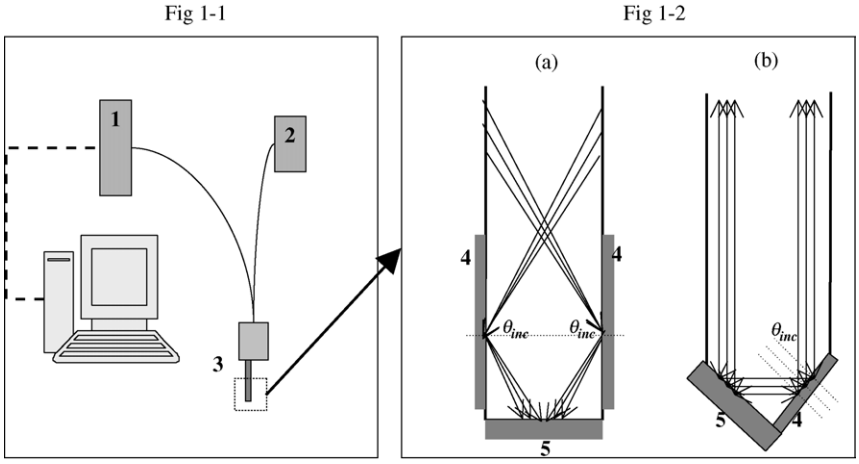

Fig. 1. Schematic diagram of experimental set-up and probe designs: (1-2a) fiber based straight SPR probe; (1-2b) fiber based tapered SPR probe. (1) spectrometer; (2) white light source; (3) SPR probe; (4) sensing surface; (5) mirror.

had 400 ± 8, 425 ± 1 and 730 ± 3 μm core, cladding and buffer diameters, respectively.

Two probe designs were selected for presentation in this paper (Fig. 1-2). In traditional straight SPR probe (Fig. 1-2a), there is not a fixed angle of incidence, but rather a range of incident angles that are allowed to propagate in the straight SPR probe. The dual-tapered SPR probe (Fig. 1-2b) has sensing surface and the front mirror polished at orthogonal angles between the two surfaces. The white light from the illuminating fiber/mirror reflects off of the tapered surfaces of the probe and is incident onto the sensing surface at the designed angle, θ_{inc}. The preparation of the sensors has been extensively described [1]. In summary the buffer and cladding are removed from the silica-fibers; the sapphire-fibers had no buffer or cladding. The fiber optic tip was polished to a desired angle with a fiber polisher (Ultra Tec). The surface was polished with 6, 3, 1 and 0.5 μm lapping films. In a modified Cressington 204 h sputter coater (Cressington), 1 nm of Cr followed by 50 nm of Au were deposited on the SPR active regions. For the rapid thermal annealing (RTA), the sapphire SPR probe was placed in a fused silica tube. After the fused silica tube was evacuated and flame-sealed, it was heated at 1200 ± 50 °C for 30 s.

2.2. Experimental design

Sixteen KCl (Fisher Scientific) solutions from 0 to 20% by mass were prepared by dilutions from a stock KCl solution. RIs of the samples were verified by an automatic digital-refractometer accurate to 0.00001 RI (A. Krüss Optronic GmbH).

A stainless steel chamber for the high-temperature and/or pressure conditions was constructed using Swagelok® components. The chamber was designed to allow the simulation of liquid sample in the seafloor hydrothermal vents. The total volume of chamber was approximately 10 mL, and pressure was attained using an HPLC sapphire piston pump (Eldex Laboratories), connected to a sample reservoir. Pressure was read from an analogue gauge incremented at 50 psi. Heating was accomplished using flexible electric heating tape (Barnstead/Thermolyne) with variable-voltage controller. The temperature was read from an internal K-type thermocouple attached to a digital thermometer (Omega), accurate to ±0.5 °C. For mounting the SPR probe into SMA, epoxy (Tra-Con, TRA-BOND F202) was generously placed on the SPR probe and SMA. This epoxy was also used to mount two fibers (illuminating and collecting optical fibers) into one steel jacket for manufacturing a bifurcated fiber optic coupler that was terminated with SMA connector. The SPR probes were linked to the coupler that was kept in alignment with the optic of the system.

For the analysis, an air reflectance spectrum was employed for the reflectance reference. Each collected spectrum was normalized to fraction reflectance across all wavelengths relative to the reference spectrum. A unique reference spectrum was collected for every sensor studied.

2.3. Data analysis

Reflectivity references were collected before each set of samples with the fiber optic sensors. References were collected in media where the SPR response would be far outside of the spectral window. Normalizing each spectrum by the appropriate reference yields the familiar SPR dip.

Observed SPR spectral features were compared to the theoretical SPR features from the model proposed by Ishimaru [22]. A Matlab (Mathworks) program was written in house to calculate the theoretical SPR response. This is the same model as was employed by Johnston et al. [23]. Note that the theoretical SPR model assumed TM polarized light while the optical fiber probes use un-polarized light. Thus, where the theoretical spectral profiles approach complete attenuation at the spectral feature, the observed spectral features would approach 50% attenuation. The non-negative least squares

fitting algorithm in Matlab was employed to fit theoretical SPR spectra to the observed SPR spectra. The fact that SPR spectra are actually attenuation from unity, not additive from a zero baseline like absorbance spectra, was accounted for in the assumed linear additive spectral mixing model.

3. Results and discussion

3.1. Limits of straight fiber optic SPR probes

SPR spectral features are readily observed in aqueous solutions using a straight silica-fiber with the cladding and buffer removed [1]. In this most recent work, 0.39 NA TECS^{TM} clad multimode silica-fibers were used for manufacturing the straight SPR probes. The SPW is excited at many angles simultaneously and the SPR spectrum is accumulated spectra of the entire range of the propagating angles, from 70° to 89°. Thus the observed SPR spectral feature is broader than commonly seen with single angle prism-based SPR systems.

The SPR dip is not observed with the straight core-only sapphire probes. The sapphire core has a refractive index ~1.76; thus the theoretical NA of the fiber in aqueous solution is approximately 1.45. Therefore, this would suggest that any angle on the input face of sapphire-fiber would be transmitted. However the theoretical NA of a sapphire-fiber is significantly larger than the functional NA because of light scattering from defects on large acceptant angles [24]. As a result an effective numerical aperture, NA_{eff} has been applied in this case. The NA_{eff} is defined as the sine of the launch angle at which the transmission drops to 50% of the transmission with a 0° of launch angle. In this study, the NA_{eff} of multimode sapphire-fiber used for SPR probe manufacture is 0.12. Therefore, the sapphire-fiber supports internal propagating angles of light from 83° to 90°. Within this incident angular region, wavelength required to excite the SPW does not fall within the spectral range covered by the system used. Fig. 2b illustrates the normalized SPR spectrum of 10% KCl solution in straight sapphire-fiber based SPR probe. The theoretical (Fig. 2a) and experimental (Fig. 2b) spectra are in good agreement with one another. As a result, the SPW could not be produced on the range of internal incident angles, 83°–89° in sapphire-fiber SPR probe. The attenuation observed below 600 nm is non-SP based attenuation predicted by the Fresnel equations.

3.2. Sapphire tapered fiber optic SPR probes for aqueous phase RI monitoring

The incident angle of tapered sapphire-fiber optic probe is optimized in design for exciting SPR. The light reflects off the tapered side at the designed angle and is directed back in parallel to the incident light through the mirror. The light from the mirror is also reflected off the tapered side with the same incident angle. The sensing surface was prepared by successive vacuum deposition of chromium (thickness, 1 nm) and gold (thickness, 50 nm) after thoroughly cleaning the fiber. The mirror was fabricated with reflective metals, chromium and gold deposited onto the region with such thickness greater than 200 nm so as not to excite SPR.

Fig. 3b illustrates the measured SPR spectral features of three dual-tapered probes with 57°/33°, 59°/31°, and 61°/29° (i.e., θ_{inc} @ sensing surface/θ_{inc} @ mirror) in a 5 wt.% KCl solution. The light is incident upon the mirrors as well, but SPR on the mirrors is not activated because of their thick thickness. The distribution of angles propagating in a sapphire-fiber has a mean too far from normal to make an effective fiber optic SPR sensor for monitoring the RI of aqueous solutions without tapering the fiber tip to bring the angle of incidence at the SPR sensing region nearer to normal. The Fresnel equations predict that a 61°–57° angle of incidence is required to observe the SPR attenuation with the materials employed to construct the sapphire based probes

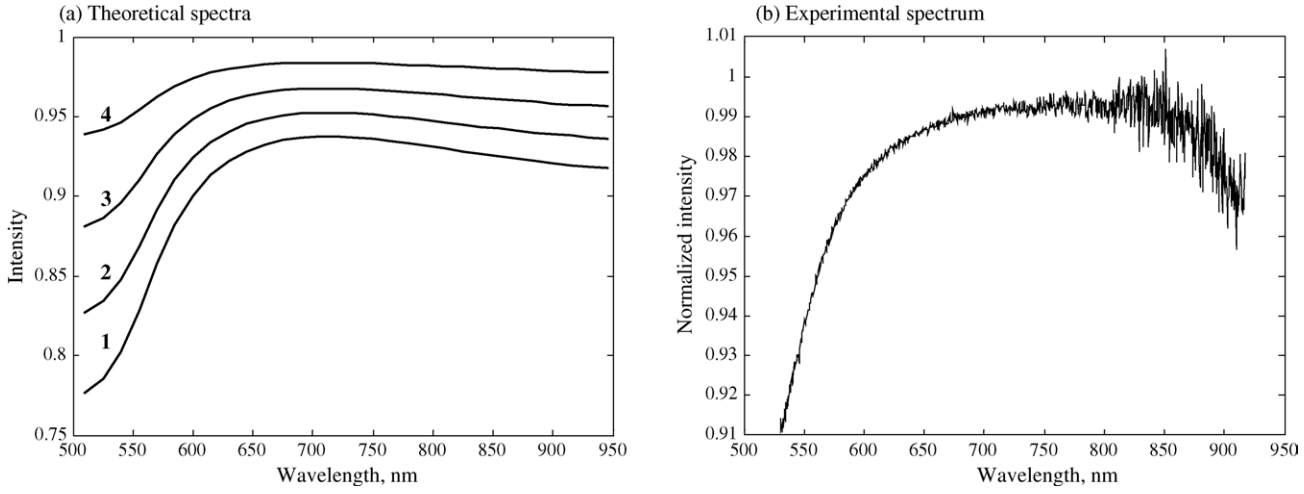

Fig. 2. SPR spectra from straight sapphire-fiber SPR probe. Medium, 10% KCl solution in water (RI, 1.35148 at room temperature): (1) θ_{inc} = 86°; (2) θ_{inc} = 87°; (3) θ_{inc} = 88°; (4) θ_{inc} = 89°; Kaiser Hollospec spectrograph with 449.61 nm of spectral coverage; the atmosphere and room temperature.

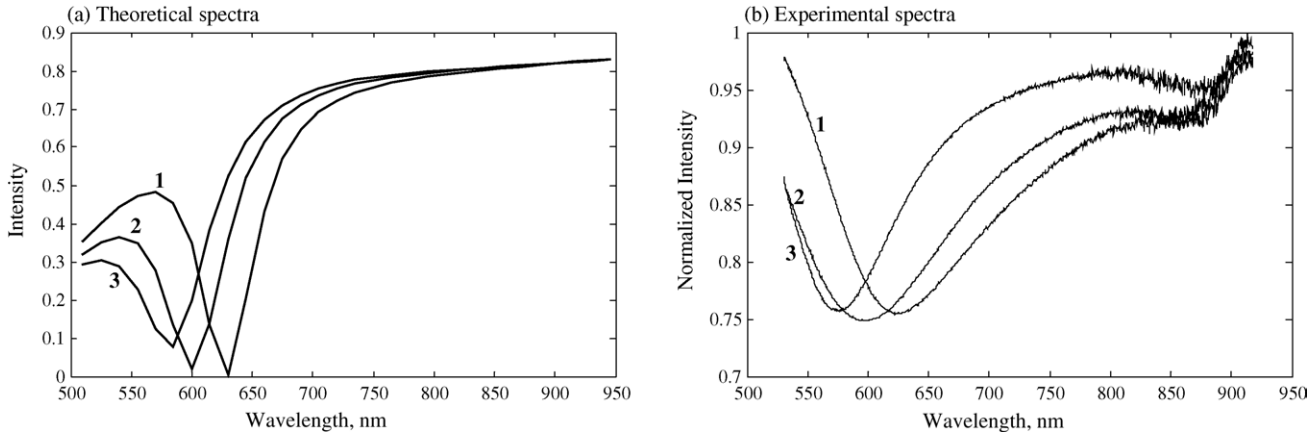

Fig. 3. SPR spectra from tapered sapphire-fiber SPR probe (three angles and one RI). Medium, 5% KCl solution in water (RI, 1.34570 at room temperature): (1) $\theta_{inc} = 57°$; (2) $\theta_{inc} = 59°$; (3) $\theta_{inc} = 61°$; Kaiser Hollospec spectrograph with 449.61 nm of spectral coverage; the atmosphere and room temperature.

(Fig. 3a). Tapering the sapphire-fibers such that the angle of incidence on the tip is between 57° and 61° does return a useful SPR spectral feature in qualitative agreement with the theoretical SPR spectrum. However, the observed spectral feature is much broader than the theoretical spectrum due to the fact that the wavelength of maximum attenuation is very sensitive to imperfections in collimating the light when such steep angles of incidence are employed.

Three bases set of 1024 theoretical SPR spectra from angles of incidence between 56° and 58°, 58° and 60°, and 60° and 62° were employed to model the specrum for a sample RI of 1.34570 (5% KCl solution). In the model a four layer sapphire/chromium (1 nm)/gold (50 nm)/media (infinite) system was assumed. The complex permittivities of gold, chromium, and sapphire were employed from literature values [25] and interpolated based on a fifth order polynomial [1]. The non-negative-least squares optimization algorithm converged to each basis set of spectra to fit the observed curve (Fig. 4). The distribution of the least squares fitting spectra (smoothing lines) is close to the measured spectral feature. The models show significant contribution in the observed SPR spectra from propagating modes as far away as 2° from the main SPR active mode. This effect is a direct result of the narrow distribution of modes propagating down the 0.12 effective NA fiber and the inability to accurately and precisely polish the sensing surface. For example, the fiber targeted to polish at 61° has its main contribution from a mode contacting the SPR active surface at 62.8° incident from the fiber walls.

Based on the theoretical spectra predicted by the Fresnel equations, three bare sapphire SPR probes were constructed with tapered tips of 57°/33°, 59°/31°, and 61°/29°, such that the sensors would be responsive to RI changes between distilled water and sea water (3.5% salinity). The observed SPR features agree qualitatively with the predicted spectra (Fig. 5). The probes were tested with six KCl solutions (0, 1, 5, 10, 15, 20 wt.% KCl in distilled water) ranging from 1.33315 to 1.35756 RI. All three probes have essentially the same theoretical and observed sensitivity (wavelength shift per change in RI) over this range, but the standard deviation of 50 replicate measurements for the 57°/33° bare sapphire sensor (0.06–0.19 nm for the six samples) is significantly greater than the standard deviation for the 59°/31° (0.02–0.08 nm) and the 61°/29° (0.01–0.03 nm) configurations. The difference in precision of estimating the wavelength position of the SPR can largely be explained by the relative widths of the SPR features from the three sensors. The 57°/33° configuration has much broader dips due to the angular sensitivity on the incident photons; thus any movement in the fibers that effect change in the distribution of light at the fiber jumper—sensor interface is more likely to slightly change the observed SPR feature.

The magnitude of difference between data points of SPR coupling wavelength and their first-order polynomial fittings is illustrated in Fig. 6. The residuals of theoretical model were significantly less than that of the experiment, and the residuals from experimental data were in ±1 nm. In the practical experiment, the reflection occurring at interfaces such as the coupler|air|SPR probe will increase the background light intensity of the measured light, thus decreasing the SPR coupling efficiency. Also, it is possible for the angular and linear offset to mismatch between coupler and SPR probe, thus the SPR probes will not introduce parallel rays of light, which will not properly be coupled back into the coupler.

3.3. Fiber optic SPR probes in the hydrothermal fluids

Rapid thermal annealing (RTA) was found to improve the sharpness of the SPR spectral features. Fig. 7 shows typical observed SPR features for the 59°/31° configuration for a Sapphire SPR sensor before and after RTA. For SPR analysis, narrow and deep features are considered preferable to broad, shallow spectral features. Thus, the aspect ratio of feature depth divided by feature width at half depth can be used to compare multiple methods of sensor preparation. Before RTA the sapphire-fiber returned spectra with an aspect of 0.000742

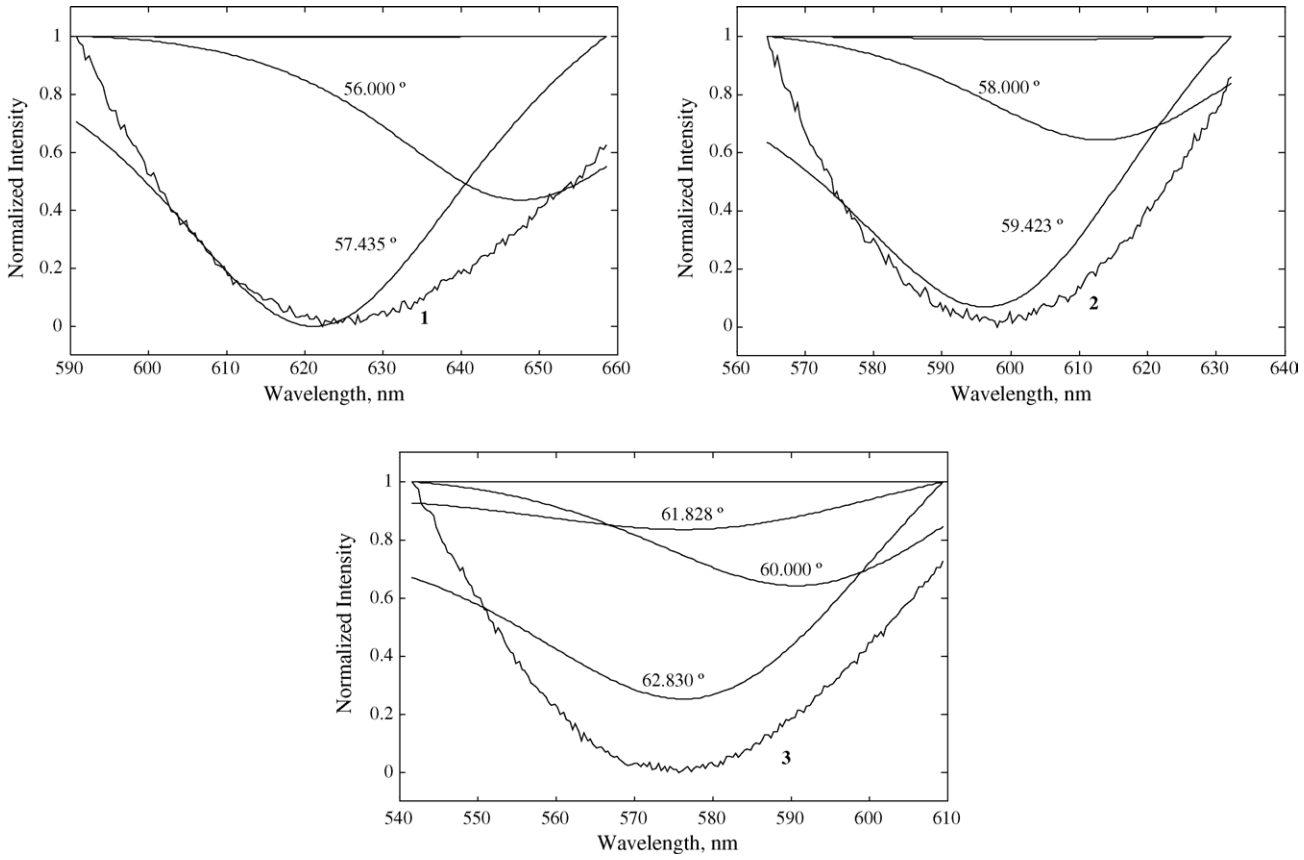

Fig. 4. Least squares fitting SPR spectra due to incidence angle. Medium, 5% KCl solution in water (RI, 1.34570 at room temperature); Sapphire-fiber based tapered probes: (1) $\theta_{inc} = 57^{\circ}$; (2) $\theta_{inc} = 59^{\circ}$; (3) $\theta_{inc} = 61^{\circ}$; the atmosphere and room temperature.

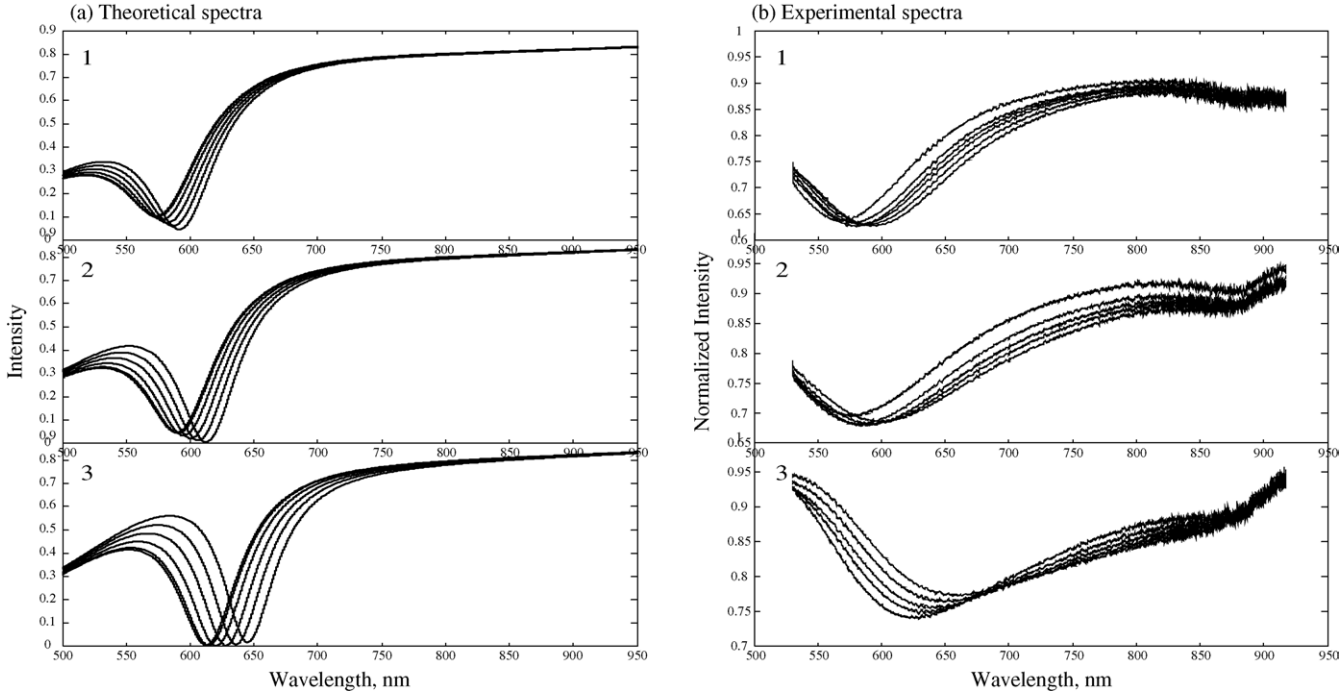

Fig. 5. SPR spectra from tapered sapphire-fiber SPR probe (three angles and six RIs). Mediums, water (RI, 1.33315), 1% (RI, 1.33458), 5% (RI, 1.33956), 10% (RI, 1.34571), 15% (RI, 1.35148), and 20% KCl (RI, 1.35756) solutions in water; Sapphire-fiber based tapered probes: (1) ($\theta_{inc} = 61^{\circ}$); (2) ($\theta_{inc} = 59^{\circ}$); (3) ($\theta_{inc} = 57^{\circ}$); Kaiser Hollospec spectrograph with 449.61 nm of spectral coverage; the atmosphere and temperature, 20 °C.

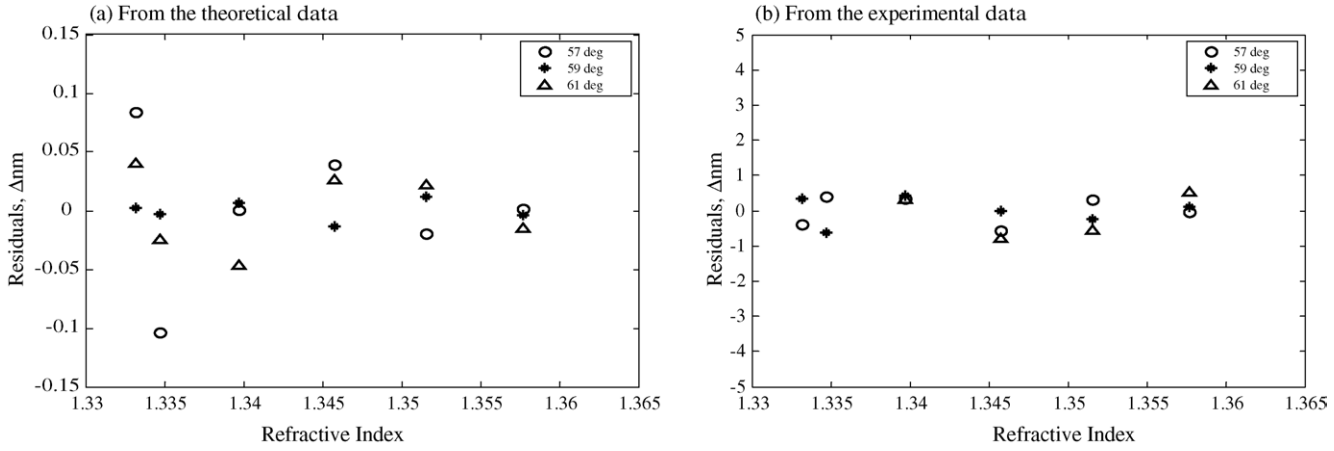

Fig. 6. Residuals of SPR coupling wavelength responses as a function of RI of mediums. Mediums, water (RI, 1.33315), 1% (RI, 1.33458), 5% (RI, 1.33956), 10% (RI, 1.34571), 15% (RI, 1.35148), and 20% KCl (RI, 1.35756) solutions in water; Sapphire-fiber based tapered probes; (1) ($\theta_{inc} = 61°$); (2) ($\theta_{inc} = 59°$); (3) ($\theta_{inc} = 57°$); the atmosphere and temperature, 20 °C.

(dip/full width at half minimum) while after RTA the aspect improved to 0.00106 (dip/full width at half minimum). This is an improvement of 29%. The improvement in SPR feature characteristics might be caused by the relatively smooth surface of gold and forming of shallow junction (Al_2O_3|Cr).

The sapphire sensors followed by RTA are capable of monitoring the RI of hydrothermal (high-temperature and pressure) fluids where silica-fibers fail. It is well know that silica is dissolved by hydrothermal water. Even coating the sensor with gold (inert to hydrothermal water) will not prevent the fiber degradation. Fig. 8d shows the silica-fiber based SPR spectral feature from hydrothermal fluid at 3000 psi as the temperature is increased from 220 to 260 °C. As the silica-fiber degrades as a function of exposure time to different hydrothermal conditions, the gold flakes off and the core becomes pitted and opaque. Consequently the reflected light decreases as the fiber degrades (Fig. 8c). A plot of SPR coupling wavelengths versus pressure/temperature for the selected experiments is linear (Fig. 8a and b). As the temperature of samples is increased, the density decreases, leading to a subsequent increase in the velocity of radiation and a decrease in the measured refractive index (i.e., SPR coupling wavelength). Also, the SPR coupling wavelength has red shift as pressure increases, due to the resulting increase in density. The relation between refractive index (n) and density (ρ) is most accurately given by the Lorentz–Lorenz expression:

$$\frac{RD}{M}\rho = \frac{n^2 - 1}{n^2 + 2}, \quad (1)$$

where RD is the molar refraction and M is the molecular weight. The RD is nearly constant with changes in temperature and pressure by virtue of the density factor, which is a function of pressure and temperature. Therefore, the refractive index is affected by changes in temperature, pressure, and sample's concentration. From the Lorentz–Lorenz formular, the refractive index has linearity to the density. The linearity of the data (Fig. 8a and b) is consistent with the Lorentz–Lorenz formular.

The sapphire-fiber based SPR probe, after the RTA, was exposed to hydrothermal water. **J**obin-SPEX 270 M spectrometer with 42.80 nm of spectral coverage has been employed for these experiments. The plot of SPR coupling wavelengths versus pressure/temperature using the sapphire-fiber based tapered SPR probe is also linear, as can be seen in Fig. 9a and b. Additionally, this data can be used to predict the changes of RI at some other pressure and temperature conditions. The RMSE of pressure calibration in hydrothermal water, 5 and 10% KCl solutions is 255.90, 170.07, and 120.37 psi, respectively. In the temperature calibrations, the RMSE of hydrothermal water, 5 and 10% KCl solutions is 3.17, 4.89, and 8.34 °C, respectively. When the sapphire-fiber

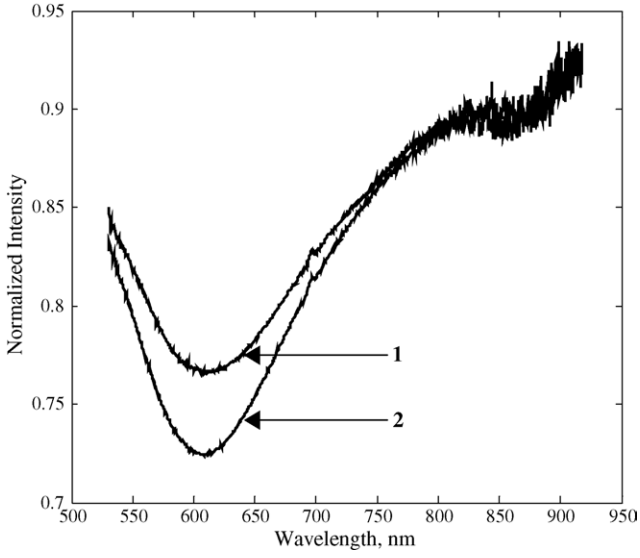

Fig. 7. Effects of rapid thermal annealing (RTA) on SPR spectra. Medium, water; (1) before RTA treatment; (2) after RTA treatment; Sapphire-fiber based tapered probe (Cr, 3 nm + Au, 43 nm and ($\theta_{inc} = 59°$)); Kaiser Hollospec spectrograph with 449.61 nm of spectral coverage; the atmosphere and room temperature.

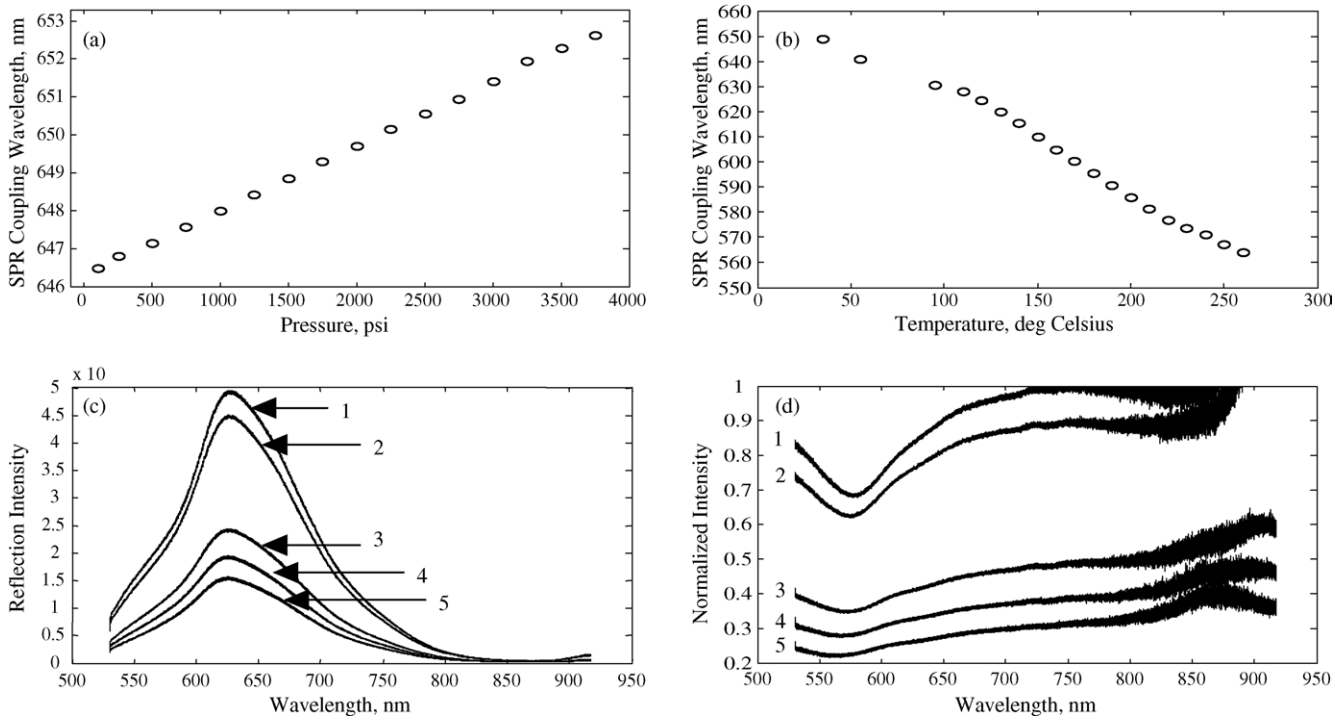

Fig. 8. Silica-fiber based SPR spectra due to pressure and temperature. Silica-fiber based straight probe without RTA treatment. Medium, 5% KCl solutions in water: (a) pressure effect at room temperature; (b) temperature effect at 3000 psi; (c) unprocessed reflection spectra as a function of temperature: (1) 220 °C; (2) 230 °C; (3) 240 °C; (4) 250 °C; (5) 260 °C; (d) normalized SPR spectra as a function of temperature: (1) 220 °C; (2) 230 °C; (3) 240 °C; (4) 250 °C; (5) 260 °C; Kaiser Hollospec spectrograph with 449.61 nm of spectral coverage.

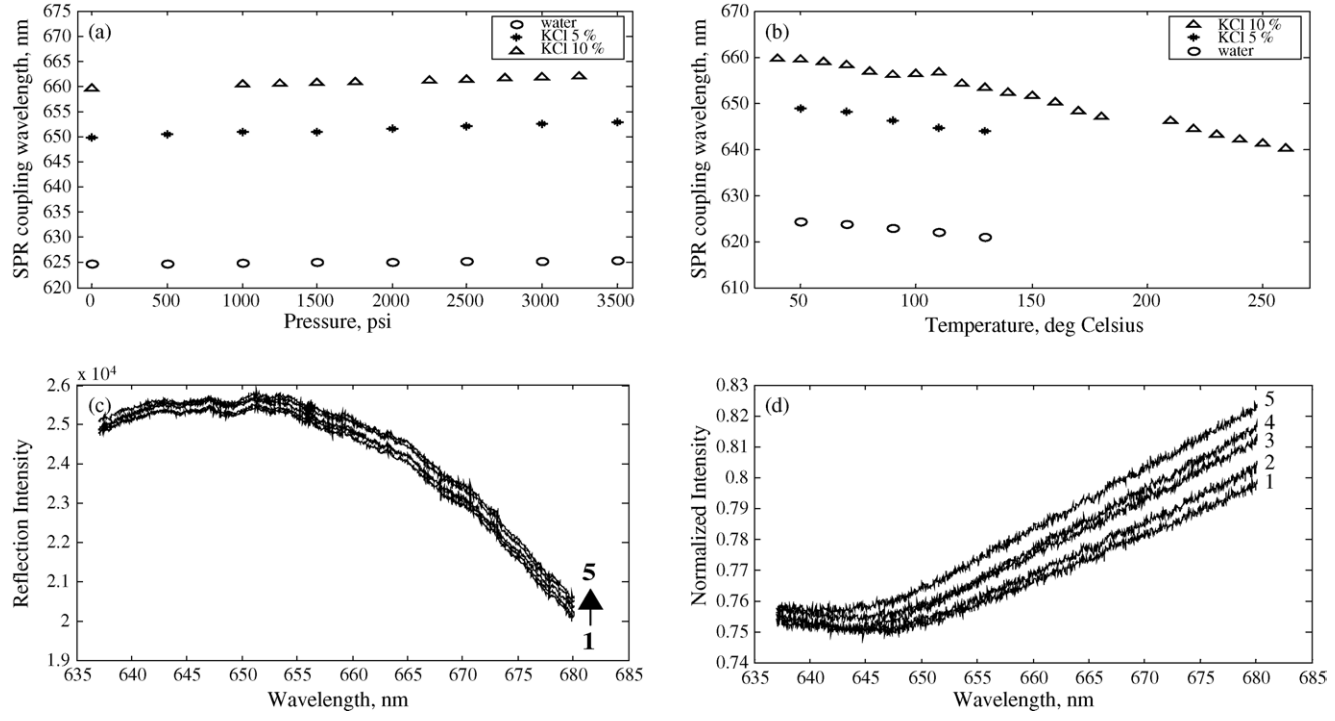

Fig. 9. Sapphire-fiber based SPR spectra due to pressure and temperature. Sapphire-fiber based tapered probe ($\theta_{inc} = 57°$) with RTA treatment. Mediums, water, 5%, and 10% KCl solutions in water: (a) pressure effect at room temperature; (b) temperature effect at 3000 psi; (c) unprocessed reflection spectra as a function of temperature: (1) 220 °C; (2) 230 °C; (3) 240 °C; (4) 250 °C; (5) 260 °C; (d) normalized SPR spectra as a function of temperature: (1) 220 °C; (2) 230 °C; (3) 240 °C; (4) 250 °C; (5) 260 °C; Jobin-SPEX 270 M spectrometer with 42.80 nm of spectral coverage.

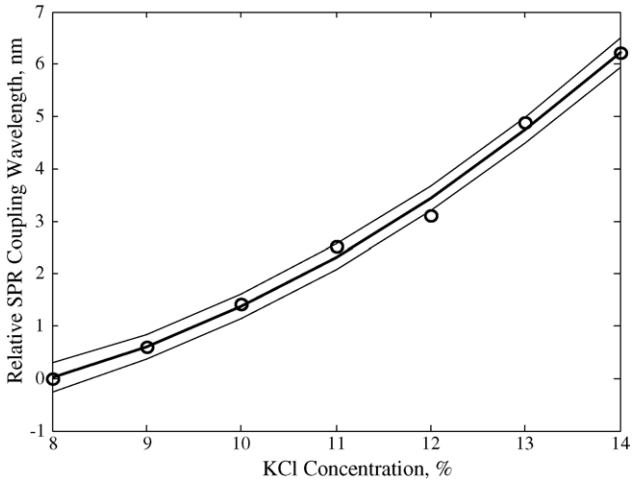

Fig. 10. Calibration curve at high pressure and temperature. Sapphire-fiber based tapered probe ($\theta_{inc} = 57°$) after RTA treatment; thicker line, second-order polynomial fitting; mediums, 8%, 9%, 10%, 11%, 12%, 13%, and 14% KCl solutions in water; pressure, 3000 psi and temperature, 250 °C.

based SPR probes after the RTA were applied to monitor RIs of KCl solutions at each temperature in 3000 psi, the intensities of reflection spectra were not loss until 260 °C (Fig. 9c). Consequently, the SPR dips were stable (Fig. 9d), and have blue shift as temperature increases.

A quantitative study of sapphire-fiber based SPR sensor at high-temperature (250 °C) and pressure (3000 psi) was performed. The calibration curve for seven KCl samples is shown in a plot sample's concentration versus relative SPR coupling wavelength (Fig. 10). Each data point (circle) was calculated by average of 50 SPR coupling wavelengths from each sample. Examination of the calibration data shows that the experimental data points fit a curve (solid line) in the range of 8–14% KCl concentrations. An equation of the fitting curve is:

$$\Delta\lambda_{SPR} = 0.0894\,\Delta C^2 - 0.935\,\Delta C + 1.78, \quad (2)$$

where $\Delta\lambda_{SPR}$ is the SPR coupling wavelength increase in nm, ΔC is the KCl concentration increase in percentage. The RMSE of calibration across the range of 8.00–14.00% KCl solutions is 0.138% KCl. The error bounds (broken lines) were produced by an interval of ±RMSE.

The sapphire-fiber SPR sensor was stable throughout all the experiments without loss of reflectivity or degradation of the SPR aspect. The stability of the sapphire was tested up to 3750 psi and 260 °C. Temperature above 260 °C was not tested because the epoxy (Tra-con, TRA-BOND F202) employed to mount the sapphire sensor in the swagelok fitting for the hydrothermal reactor is only rated to 265 °C. Pressures above 3750 psi could not be maintained in the hydrothermal system; therefore more extreme systems were not tested. In total the sapphire-fiber was exposed to hydrothermal conditions (arbitrarily defined as greater than 3000 psi and 200 °C) for more than 7 h during 14 days compared to 1 h for the silica-fiber sensor.

4. Concluding remarks

A simple and rapid method for the evaluation of RIs in harsh environment was developed. This method is based on the sapphire-fiber with SPR spectroscopy. The sapphire-fiber based SPR sensor has advantages, such as short analysis time and simplicity of use. Additionally, the applied sapphire-fiber based SPR sensor could detect changes of SPR coupling wavelength at high pressure and temperature. In view of these facts, the sapphire-fiber based SPR sensors can be considered a valuable approach for in situ, real time RIs monitoring in the harsh environment conditions.

Our current work is focusing on applying the rapid thermal annealing to sapphire-fiber SPR probes for the evaluation of stability and sensitivity. This study is currently in progress and will be reported at a later date.

Acknowledgments

This research work was supported by NSF Oceans 0119999. The authors thank Dr. Dong-Kyun Seo for providing the rapid thermal annealing system.

References

[1] L.A. Obando, K.S. Booksh, Anal. Chem. 71 (1999) 5116.
[2] L.S. Jung, C.T. Campbell, T.M. Chinowsky, M.N. Mar, S.S. Yee, Langmuir 14 (1998) 5636.
[3] M.D. Malinsky, K.L. Kelly, G.C. Schatz, R.P.V. Duyne, J. Am. Chem. Soc. 123 (2001) 1471.
[4] H.E.d. Bruijn, B.S.F. Altenberg, R.P.H. Kooyman, J. Greve, Opt. Commun. 82 (1991) 425.
[5] E. Kretschmann, Zeitschrift fuer Physik 221 (1969) 346.
[6] E. Kretschmann, Zeitschrift fuer Physik 221 (1969) 357.
[7] K.S. Johnston, S.S. Yee, K.S. Booksh, Anal. Chem. 69 (1997) 1844.
[8] J.-F. Masson, L.A. Obando, S. Beaudoin, K.S. Booksh, Talanta 62 (2004) 865.
[9] L.A. Obando, D.J. Gentleman, J.R. Holloway, K.S. Booksh, Sens. Actuators B 100 (2004) 439.
[10] D.J. Gentleman, L.A. Obando, J.-F. Masson, J.R. Holloway, K.S. Booksh, Anal. Chim. Acta 515 (2004) 291.
[11] J.-F. Masson, T.M. Battaglia, Y.-C. Kim, A. Prakash, S. Beaudoin, K.S. Booksh, Talanta 64 (2004) 716.
[12] J.-F. Masson, M. Barnhart, T.M. Battaglia, G.E. Morris, R.A. Nieman, P.J. Young, C.L. Lorson, K.S. Booksh, Analyst 129 (2004) 855.
[13] J.-F. Masson, T. Hartmann, H. Dürr, K.S. Booksh, Opt. Mater. 27 (2004) 435.
[14] M. Niggemann, A. Katerkamp, M. Pellmann, P. Bolsmann, J. Reinbold, K. Cammann, Sens. Actuators B 34 (1996) 328.
[15] A. Diez, M.V. Andres, J.L. Cruz, Sens. Actuators B 73 (2001) 95.
[16] R.C. Jorgenson, Sens. Actuators B 73 (2001) 236.
[17] C.P. Cahill, K.S. Johnston, S.S. Yee, Sens. Actuators B 45 (1997) 161.
[18] R.C. Jorgenson, S.S. Yee, Sens. Actuators A 45 (1994) 44.
[19] D.J. Fornari, T. Shank, K.L. Von Damm, T.K.P. Gregg, M. Lilley, G. Levai, A. Bray, R.M. Haymon, M.R. Perfit, R. Lutz, Earth Planet Sci. Lett. 160 (1998) 419.

[20] K. Ding, W.E. Seyfried, M.K. Tivey, A.M. Bradley, Earth Planet Sci. Lett. 186 (2001) 417.
[21] T.F. Rozan, S.M. Theberge, G. Luther, Anal. Chim. Acta 415 (2000) 175.
[22] A. Ishimaru, Electromagnetic Wave Propagation, Radiation, and Scattering, Prentice-Hall, New Jersey, 1991 (Chapter 3).
[23] K.S. Johnston, S.R. Karlsen, C.C. Jung, S.S. Yee, Mater. Chem. Phys. 42 (1995) 242.
[24] R.K. Nubling, J.A. Harrington, Appl. Opt. 36 (1997) 5934.
[25] E.D. Palik, Handbook of Optical Constants of Solids, Academic Press, New York, 1985.